Author Manuscript

Author Manuscript

Author Manuscript

Author Manuscript

HHS Public Access

Author manuscript

Hepatology. Author manuscript; available in PMC 2017 February 01.

Published in final edited form as:

Hepatology. 2016 February ; 63(2): 512–523. doi:10.1002/hep.27973.

Pharmacological inhibition of ASBT changes bile composition and blocks progression of sclerosing cholangitis in mdr2 knockout mice

Alexander G Miethke[1,5], **Wujuan Zhang**[2], **Julie Simmons**[1], **Amy Taylor**[1], **Tiffany Shi**[1], **Shiva Kumar Shanmukhappa**[2], **Rebekah Karns**[3], **Shana White**[3], **Anil G Jegga**[3,5], **Celine S Lages**[1], **Stephenson Nkinin**[2], **Bradley T Keller**[4], and **Kenneth D. R. Setchell**[2,5]

[1]Division of Pediatric Gastroenterology, Hepatology, and Nutrition, Cincinnati Children's Hospital Medical Center, Cincinnati, Ohio

[2]Division of Pathology and Laboratory Medicine, Cincinnati Children's Hospital Medical Center, Cincinnati, Ohio

[3]Division of Biomedical Informatics, Cincinnati Children's Hospital Medical Center, Cincinnati, Ohio

[4]Consultant to Shire plc., San Diego, CA

[5]Department of Pediatrics, University of Cincinnati College of Medicine, Cincinnati, Ohio, USA

Abstract

Deficiency for mdr2, a canalicular phospholipid floppase, leads to excretion of low phospholipid "toxic" bile causing progressive cholestasis. We hypothesize that pharmacological inhibition of the ileal apical sodium-dependent bile acid transporter (ASBT) blocks progression of sclerosing cholangitis in mdr2−/− mice. 30-day-old, female mdr2−/− mice were fed high-fat chow containing 0.006% SC-435, a minimally absorbed, potent inhibitor of ASBT, providing on average 11 mg/kg/day of compound. Bile acids (BA) and phospholipids were measured by mass spectrometry. Compared with untreated mdr2−/− mice, SC-435 treatment for 14 days increased fecal BA excretion by 8-fold, lowered total BA concentration in liver by 65%, reduced total BA

Contact Information: Alexander G Miethke, MD, Assistant Professor of Pediatrics, Pediatric Gastroenterology, Hepatology, and Nutrition, MLC 2010, Cincinnati Children's Hospital Medical Center, 3333 Burnet Avenue, Cincinnati, OH 45229, Phone: 513.636.8948, Fax: 513.636.5581, alexander.miethke@cchmc.org.

Disclosure of personal and financial conflicts of interests

Alexander G Miethke, MD; received unrestricted Industry research grant (>$5,000) to CCHMC from Lumena Pharmaceutical Inc. and "PSC-Partners seeking a cure"; obtained funding, designed the experiments, was responsible for analysis and interpretation of the data, and drafting of the manuscript

Kenneth D. R. Setchell, PhD[2,5]; Principle Investigator on Industry Grants awarded to CCHMC for analysis of samples from Lumena sponsored clinical trials of ASBT inhibitors (>$5,000) and received a travel grant for attendance and presentation of data at an international congress ($3,000); A Member of the Board of Managers and minor equity holder in Asklepion Pharmaceuticals, LLC; Consultant to NGM Biopharmaceuticals Inc., (<$5,000); responsible for the conception and design of bile acid and lipid studies, developed sterol and bile acid assays, interpreted LC-MS data, and critical revision of the manuscript for important intellectual content.

All other authors declare no potential conflicts of interest.

Prior presentation of experimental data:

This paper was presented in part at the FALK symposium on "Bile Acids as Signal Integrators and Metabolic Modulators" in Freiburg, Germany, 2014, at the Biliary Atresia and Related Diseases Meeting in Berlin, Germany, 2014, and at the 65th AASLD Annual Meeting in Boston, MA, 2014.

Author Manuscript Author Manuscript Author Manuscript Author Manuscript

and individual hydrophobic BA concentrations in serum by >98%, and decreased plasma ALT, total bilirubin, and serum alkaline phosphatase levels by 86, 93 and 55%, respectively. Liver histology of sclerosing cholangitis improved, and extent of fibrosis decreased concomitant with reduction of hepatic profibrogenic gene expression. Biliary BA concentrations significantly decreased and phospholipids remained low and unchanged with treatment. The phosphatidylcholine/BA ratio in treated mice corrected towards a ratio of 0.28 found in wild type mice, indicating decreased bile toxicity. Hepatic RNAseq studies revealed upregulation of putative anti-inflammatory and antifibrogenic genes, including *Ppara* and *Igf1* and downregulation of several pro-inflammatory genes, including *Ccl2* and *Lcn2*, implicated in leukocyte recruitment. Flow cytometric analysis revealed significant reduction of frequencies of hepatic $CD11b^{+}F4/80^{+}$ Kupffer cells and $CD11b^{+}Gr1^{+}$ neutrophils, accompanied by expansion of anti-inflammatory $Ly6C^{-}$ monocytes in treated mdr2−/− mice.

Conclusion—Inhibition of ASBT reduces BA pool size and retention of hydrophobic BA, favorably alters the biliary PC/BA ratio, profoundly changes the hepatic transcriptome, attenuates recruitment of leukocytes, and abrogates progression of murine sclerosing cholangitis.

Keywords

primary sclerosing cholangitis; SC-435; cholestasis; liver fibrosis; bile acid signaling

Introduction

Chronic fibrosing cholangiopathies, like progressive familial intrahepatic cholestasis (PFIC) type 3, biliary atresia or primary sclerosing cholangitis (PSC), carry high morbidity and mortality due to complications from progressive cholestasis and fibrosis. Cholestasis in these conditions often results from impaired hepatocellular and bile duct epithelial excretion of bile constituents, primarily bile acids (BA), phospholipids (PL) and cholesterol, and from ductal obstruction of bile flow. Bile duct epithelial cells become injured which leads to upregulation of adhesion molecules, secretion of pro-inflammatory cytokines and chemokines, and ultimately recruitment of leukocytes to the portal tract driving the fibro-obliteration of the biliary tree, as previously reviewed for cholestatic disorders and their animal models (1, 2). Formation and retention of “toxic” BA likely play important roles in perpetuating the disease process (3). For instance, hydrophobic BA species are known to trigger hepatobiliary inflammation and to cause hepatocyte death by apoptosis (4). Further evidence for the pathogenic role of BAs in cholangiopathies originates from genome-wide association studies on patients with PSC which identified not only genes linked to the HLA complex but also *GPBAR1* encoding the BA receptor TGR5 as possible disease genes (5). Among many functions, TGR5 has been implicated in regulating production of pro-inflammatory cytokines by macrophages (6).

The multidrug resistance gene 2 knockout mouse (mdr2−/−) represents an established animal model for chronic cholestatic disorders, especially progressive familial intrahepatic cholestasis (PFIC) type 3 (7) and may recapitulate some aspects of the pathogenesis of PSC (8). These mice display absence of PL from bile (9) which disrupts the formation of mixed micelles and subsequently leads to “toxic bile” triggering an inflammatory cascade (10). This model has been extensively used for preclinical studies of novel therapies for chronic

Author Manuscript Author Manuscript Author Manuscript Author Manuscript

cholestasis, targeting anticholestatic, anti-inflammatory and antifibrogenic pathways (11, 12) .

BA homeostasis is tightly regulated through *de novo* synthesis from cholesterol in the liver, efficient re-uptake of BAs in the distal small intestine, and feedback regulation of hepatic *de novo* synthesis through the BA-FXR-fibroblast growth factor FGF19 (Fgf15 in mice) signaling pathway. BAs act through FXR in ileal enterocytes and induce expression of the hormone FGF19/15 which subsequently binds to the receptor complex FGFR4-β-Klotho on the surface of hepatocytes resulting in repression of Cyp7A1 mediated BA synthesis. Less than 5% of the circulating BA pool typically escapes reabsorption and is eliminated in the feces on a daily basis. The majority of BAs are absorbed via active transport in the terminal ileum, mediated by the *ABCB4* encoded apical sodium-dependent bile acid transporter (ASBT). The compound SC-435 is a specific, non-absorbable, inhibitor of ASBT and BA reuptake in the distal ileum (13). Consequently, we hypothesized that inhibiting the enterohepatic circulation of BAs by pharmacologically blocking ASBT with SC-435 would diminish the BA pool size and attenuate progression of sclerosing cholangitis in the mdr2−/− mouse model of chronic cholestasis.

Material and Methods

Mice

Mdr2−/− mice in BALB/cJ background were a generous gift from Prof. Lammert (Homburg University, Germany) and wild type BALB/cJ mice were purchased from Charles River Laboratories. All mice were bred in house and kept in conventional conditions. 30-day-old, female mdr2−/− and wild type mice were treated with 0.006% SC-435 admixed to high-fat breeder chow (Mouse diet 5020 with 9% fat, Cincinnati Lab Supply, OH) for 14 days until the time of harvest, providing approximately 11 mg/kg/day of the compound. Control mice were treated under identical conditions, but received Lab 5020 chow without the compound. All protocols were approved by the Animal Care and Use Committee of the Cincinnati Children's Research Foundation.

Fecal BA

Mice were single-housed on raised, wire-bottom cages for 48 hours prior to collection of all fecal material, which was re-hydrated with water equal to 2 times the total fecal weight, overnight at 4°C. BAs were extracted with 50% v/v t-butanol/water (v/v) for 45 minutes at 37 °C, centrifuged at 2000*g* for 15 minutes. BA concentration was determined using the Diazyme Total Bile Acids Universal (enzymatic) kit and read on a BioTek Synergy H1 Plate Reader.

Plasma and serum biochemistries

Plasma total bilirubin and alanine aminotransferase (ALT) levels were determined as reported before (14). Serum alkaline phosphatase (ALP) concentration was measured using DISCRETPAK reagents from Catachem (C174-0C).

Author Manuscript Author Manuscript Author Manuscript Author Manuscript

Analysis of BA, PL, cholesterol and C4 concentrations by liquid chromatography-mass spectrometry (LC-MS)

Quantitative analysis of BA, PL and cholesterol was carried out using a Waters API triple quadruple mass spectrometer interfaced with Aquity UPLC system (Milford, MA). Serum and biliary BAs were extracted on a reverse phase solid phase cartridge. Liver tissue was exhaustively extracted with organic solvents before aqueous dilution and solid-phase extraction. Bile acids in the biological samples were quantified against curves constructed for the 15 most common endogenous BAs based on a stable-isotope dilution analysis with single ion recording-mass spectrometry (SIR-MS)(15). PLs were extracted by the Folch procedure and quantified using phosphatidylcholine (PC) standards based on mass spectrometry with multiple reactions monitoring (MRM) function. Total PL was calculated based on the summation of 13 major PC species detected in serum or bile. Bile samples were treated with alkaline hydrolysis to measure the total cholesterol concentrations by an isotope dilution APCI-LC-MS method. Plasma 7α-hydroxy-4-cholesten-3-one (C4) concentration was determined by a validated stable-isotope dilution tandem mass spectrometry using deuterium labeled 7α-hydroxy-4-cholesten-3-one ([$^2H_7$-25,26,26,26,27,27,27]-7α-hydroxy-4-cholesten-3-one, D_7-C4) as internal standard.

Quantitative Real-Time PCR

Total RNA was isolated from liver tissue, reverse-transcribed, and mRNA concentration of *TNFα* was determined by SYBR green qPCR. *SMA (Acta2)* and *TIMP1* genes were amplified using TaqMan Universal Master Mix II, with the probes Mm01546133_m1 and Mm00441818_m1, respectively, and run on Applied Biosystems 7900H Fast Real Time PCR System. The ΔΔCt method was used for computation of relative mRNA concentrations, and data were normalized to mouse *HPRT* expression.

Liver histology, ultrastructure, and Ki67 immunohistochemistry

Liver histology was blindly assessed by S.K.S. for inflammation, necrosis, bile duct proliferation, and fibrosis on a 1 to 4+ scale, as previously used in a model of obstructive cholangiopathy (16). Masson's trichrome stained liver slides were scanned using a Aperio® AT2 Digital Whole Slide scanner (Leica Microsystems Inc., Buffalo Grove, IL United States) at a resolution of 50,000 pixels per inch (0.5 μm per pixel). Pixels were classified as fibrosis (blue), liver cells (red), or background (white) by means of an image analysis algorithm as described previously (17). For electron microscopy, liver tissue was fixed in 3 % buffered glutaraldehyde, subjected to ultrathin sectioning and examined with a Hitachi H7650 transmission electron microscope. Immunohistochemistry for Ki67 was performed on paraffin embedded liver sections, using anti-mKi67 (clone SP6) following heat antigen retrieval with 1M Na Citrate (pH=6).

RNASeq and ToppGene unbiased pathway analysis

Total hepatic RNA was isolated from the caudate liver lobe. RNA-seq libraries were prepared with the Illumina TruSeq RNA preparation kit and sequenced on the Illumina Hi-Seq 2000. Sequences were aligned to the reference genome with TopHat (18) and processed with Cufflinks (19), which quantifies each transcript in each sample using reference

Author Manuscript Author Manuscript Author Manuscript Author Manuscript

annotations produced by UCSC. Differentially expressed genes with a fold change of >= 2.0 and p<0.05 between SC-435 treated and control animals were submitted to pathway enrichment analysis with ToppFun application from the ToppGene Suite, which uses unbiased methods to assess pathway enrichment (20). Raw and normalized data are accessible through NCBI's Gene Expression Omnibus (GEO accession number GSE66231). The RNAseq data can be viewed using the following link: http://www.ncbi.nlm.nih.gov/geo/query/acc.cgi?token=cjavskagdnopfmx&acc=GSE66231

Flow Cytometry

Livers were perfused with 10 ml of RPMI (Gibco) with 1 μg/ml collagenase D (Roche) prior to mechanical disruption with a Miltenyi Biotec disintegrator. Single cell preparation and staining was performed as described before (14) using the following antibodies from Biolegend (anti-mCD3-Brilliant violet 421, anti-mCD19-Brilliant violet 605), eBioscience (anti-mF4/80-PE, anti-mCD11b-PerCP-Cy5.5, anti-mGR1-APC-eFluor 780), and BD-Pharmingen (anti-mLy6C-PE-Cy7). Data were acquired on a BD Canto III and analyzed using FlowJo version 7.6.5.

Statistics

Values are expressed as mean ± standard error (SEM) and statistical significance was determined by unpaired t test, with a significance set at p<0.05. One way analysis of variance (ANOVA) with post-hoc Tukey's multiple comparison test was used to assess statistical significance between more than two groups.

Results

SC-435 increased fecal BA excretion and lowered serum BA levels

Compared with age- and gender-matched control mice receiving chow without the compound, 48 hour fecal BA excretion following 14-days treatment with SC-435 was increased by 8.6-fold in mdr2−/− and by 3.2-fold in mdr2+/+ mice (Fig 1A). Increased fecal BA losses were associated with reduction of the total BA concentration in liver tissue by 65% (Fig 1B) and a decrease in serum total BA levels by 98.9% in SC-435 treated compared with control mdr2−/− mice (Fig 1C). The major BA species, taurocholic (TCA) and tauro-β-muricholic acid (TMCA), which constituted 95.9% of the serum BA in control mdr2−/− mice, were both significantly reduced following treatment with SC-435 (Fig 1D). Importantly, the more hydrophobic BAs, taurochenodeoxycholate (TCDCA) and taurodeoxycholate (TDCA) which were significantly elevated in control mdr2−/− compared with mdr2+/+ mice (1260- and 13-fold, respectively) were significantly reduced by treatment with SC-435.

SC-435 exerted anticholestatic, anti-inflammatory and antifibrogenic effects

Altered BA homeostasis was associated with profound changes in the sclerosing cholangitis phenotype in mdr2−/− mice. Whereas control mdr2−/− mice started to lose weight after day 7 of the treatment period, those treated with SC-435 maintained weight in a similar manner to mdr2+/+ mice (Fig 2A). Furthermore, biomarkers of hepatocellular injury (plasma ALT concentration) and of cholestasis (plasma total bilirubin and serum ALP concentrations),

Author Manuscript Author Manuscript Author Manuscript Author Manuscript

which were all increased in untreated mdr2−/− mice compared with mdr2+/+ controls, were reduced in SC-435-treated mdr2−/− mice by 86, 93 and 55%, respectively (Fig 2B).

Consistent with the change in plasma biochemistries, liver histology of sclerosing cholangitis featuring periportal inflammation and fibrosis, as depicted in representative H&E and trichrome stained sections in Fig 3A, was significantly improved by SC-435 treatment. Review of histology using a previously validated sclerosing cholangitis scoring system revealed reduced scores for periportal inflammation, bile duct proliferation, necrosis and fibrosis in SC-435 treated knockout mice compared with controls (Fig 3B). Reduction in the fibrosis score was consistent with results from the Aperio-based image analysis of trichrome stained liver sections. The percentage fibrosis of total liver tissue was reduced from 4.7 to 1.6 with SC-435 treatment (Fig 3C). The histological data were corroborated by targeted gene expression studies for signature genes of sclerosing cholangitis associated hepatic inflammation (*TNFα*) and fibrosis (*SMA* and *TIMP1*). mRNA expressions for *TNFα*, *SMA* and *TIMP1* were significantly down-regulated in SC-435 versus control mdr2−/− mice (Fig 3D).

SC-435 treatment upregulated genes of BA synthesis and hepatoprotective pathways, and downregulated pro-inflammatory genes

To further probe the mechanism of action by which disruption of the enterohepatic circulation of BAs blocked progression of sclerosing cholangitis in mdr2−/− mice, we performed RNAseq studies on total liver RNA purified from SC-435-treated and control mice of both genotypes. There were 497 genes that were >2-fold upregulated by SC-435 treatment in mdr2−/− mice, of which 32 genes (6.4%) were also upregulated in SC-435 treated mdr2+/+ mice, when compared to the corresponding untreated genotype. In contrast, 332 genes were downregulated in mdr2−/− mice, of which only 3 genes (0.9%) were also downregulated in mdr2+/+ mice (Fig 4A). In an unbiased analysis, many genes related to cholesterol and BA metabolism were significantly upregulated by SC-435 treatment whereas genes in pathways related to leukocyte recruitment and function were generally downregulated when compared with untreated mdr2−/− mice (Fig 4B). Most notably, *Cyp7a1* and *Hmgcr* encoding the rate-limiting enzymes of BA and cholesterol synthesis, respectively, were upregulated by SC-435 in mice of both genotypes. Several genes encoding proteins previously implicated in protection from cholestatic injury were also upregulated in SC-435 treated mdr2−/− mice. For instance, these included *Ppara*-encoding the transcription factor Pparα, *Car1/Car3/Car5a* encoding isoforms of carbonic anhydrase, *Aqp8* encoding the water channel aquaporin 8, and *Igf1* encoding insulin-growth factor 1 (Fig 4C). Among the downregulated genes in treated mdr2−/− mice, a few related to BA and cholesterol metabolism including *Nr0b2*/Shp, the downstream messenger molecule of Fxr, and *Abcb1a/* Mdr1 and *Abcg5/* Abcg5 encoding canalicular transporters for BA and cholesterol, respectively. The majority of genes downregulated following SC-435 treatment were pro-inflammatory and profibrogenic. Highest fold-changes in differential gene expression were observed for the genes *Ccl2*, *Cxcl1*, and *Lcn2* (Fig 4C). *Tgfb1* mRNA expression was reduced by 97% in SC-435 treated vs control mdr2−/− mice (p=0.001). Expression data for candidate genes which are transcriptionally regulated by BAs through Fxr-signaling are listed in the Supplemental Table 1. For instance, SC-435 treatment was

Author Manuscript Author Manuscript Author Manuscript Author Manuscript

associated with increased hepatic expression of *Fgf15*, but did not significantly alter expression of *Abcb11*/Bsep or *Abcc2*/Mrp2 in mdr2−/− mice.

SC-435 treatment profoundly altered bile composition

Consistent with hepatic upregulation of Cyp7a1, the rate-limiting enzyme of BA synthesis, upon treatment with SC-435, plasma levels of the sterol intermediate, 7α-hydroxy-4-cholesten-3-one (C4), a surrogate marker of BA synthesis (21), were increased by 3-fold in mdr2−/− and by 10-fold in mdr2+/+ mice (Fig 5A). We next examined whether this increased synthesis resulted in higher concentrations of BA in the bile, the compartment in which low-phospholipid, non-micellar bile directly injures bile duct epithelium (9, 10). As expected, the biliary PC concentration in mdr2−/− mice was reduced to 0.29% of concentrations found in the bile of mdr2+/+ controls and did not significantly change upon treatment with SC-435 (Fig 5B). However, SC-435 treatment reduced significantly the biliary concentrations of BA and cholesterol by 98.8 and 97.6%, respectively in these mice. Therefore, despite persistence of low biliary phospholipid levels, the biliary PC/BA ratio was markedly increased in SC-435 treated mdr2−/− mice (mean 0.05±0.02), although still lower than wild type control mice (mean of 0.28±0.07), and the average coefficient of 0.30 reported for most mammals under physiologic conditions (22). Using the Wang and Carey phase diagram to describe the influence of biliary composition on cholesterol crystallization (23, 24), control mdr2−/− mice plot in the 2 phase (liquid crystal) zone A (predicting precipitation of cholesterol), whereas SC-435 treated mdr2−/− mice, like wild-type animals, plot in the 1 phase micellar zone, predicting micellar solubilization of cholesterol. Collectively, these findings suggest that SC-435 attenuates progression of sclerosing cholangitis in mdr2−/− mice by altering bile composition to reduce the “toxicity” of non-micellar bile. Therefore we next examined evidence for diminished injury to cholangiocytes in SC-435 treated mdr2−/− mice.

SC-435 treatment reduced cholangiocyte injury

Typically, acute injury to cholangiocytes is followed by regeneration, which can be labeled by the proliferation marker Ki67 (25). Proliferation of cholangiocytes was significantly increased in control mdr2−/− compared with mdr2+/+ mice by immunohistochemistry for Ki67. Reduced frequency of $Ki67^+$ cells among cholangiocytes of interlobular bile ducts in SC-435 treated vs. control mdr2−/− mice suggested reduced bile duct epithelial injury in these animals (Fig 6A). Previous studies in mdr2−/− mice revealed that injury to cholangiocytes allows leaking of BA into the periductal space, which was associated with disruption in the basement membranes surrounding the interlobular bile ducts (10). Marked improvement in ultrastructure of basement membrane of the interlobular bile duct was observed in SC-435 treated mdr2−/− mice. In treated mice, 70% of the interlobular bile ducts had continuous and intact basement membrane as opposed to only 40% in untreated mdr2−/− mice. In diseased bile ducts, the basement membrane was discontinuous and irregular to being absent in some instances (n=10 bile ducts/group; Fig 6B).

Author Manuscript Author Manuscript Author Manuscript Author Manuscript

SC-435 treatment reduced recruitment of Kupffer cells and neutrophils to the liver and promoted expansion of anti-inflammatory monocytes

Diminished leukocyte recruitment and function was an additional mechanism of action of SC-435 indicated by the global hepatic gene expression studies. A significant reduction in frequencies of F4/80^{+}CD11b^{+} Kupffer cells and Gr1^{+}CD11b^{+} neutrophils, respectively, was observed by flow cytometry in SC-435 treated vs. control mdr2−/− mice. The frequency of F4/80^{-} CD11b^{+} monocytes in mdr2−/− mice was increased upon SC-435 treatment, attributable to a rise in the anti-inflammatory subset of Ly6C^{-} monocytes in the liver, whereas the proportion of pro-inflammatory and -fibrogenic Ly6C^{+} monocytes was reduced (Fig 7).

Discussion

We have demonstrated that SC-435, a small molecule inhibitor of ASBT, increased fecal BA excretion leading to a dramatic reduction of liver and serum concentrations of BAs and biomarkers of hepatocellular and cholestatic injury in female mdr2−/− mice. This response was rapid, occurring within 14 days of treatment. Compared with control mice, body mass wasting was prevented, and progression of hepatic inflammation and fibrosis was attenuated. The mechanisms of actions of SC-435 may be pleiotropic, and some are supported by our data, including 1) a reduction of the total BA pool size and circulating hydrophobic BA, 2) a decrease of biliary BA and cholesterol concentrations rendering bile less hepatotoxic, and 3) a reduction of cholestasis associated inflammatory responses.

SC-435 has been reported to enhance fecal BA excretion in non-cholestatic rodents (26). Although ASBT is expressed in the terminal ileum of mdr2−/− in similar concentration to that of mdr2+/+ mice (27), it was unknown whether the enterohepatic reuptake of BA is depressed under cholestatic condition in these mice, thus conferring resistance to treatment with an ASBT inhibitor. Under our experimental conditions, SC-435 treatment resulted in an 8-fold increase in fecal BA excretion with a concomitant 90-fold reduction of serum BA concentrations and reduction of plasma ALT, total bilirubin, and serum ALP levels. Furthermore, fibrosis was diminished, as assessed by image analysis of trichrome stained liver sections.

We propose several mechanisms of action by which treatment with SC-435 exerts its anticholestatic, anti-inflammatory and antifibrogenic-effects in the mdr2−/− mouse model of chronic cholestasis. Based on the physicochemical properties of SC-435 having minimal intestinal absorption, we focused our investigations on the SC-435-mediated regulation of BA synthesis and composition of the hepatic and biliary pool and its downstream consequences. SC-435 treatment rapidly lowered serum total and hydrophobic BA concentrations. Hydrophobic BA have previously been linked to pathogenesis of sclerosing cholangitis especially in female mdr2−/− mice (28) and were shown to stimulate hepatocyte apoptosis through non-specific detergent effects (29), activation of death receptors (30) and induction of oxidative damage causing mitochondrial dysfunction (31). Which of these pathways is predominant in mdr2−/− mice is unknown.

Author Manuscript Author Manuscript Author Manuscript Author Manuscript

Global hepatic gene expression studies provided further insights into effects of SC-435 treatment on putative mechanisms of action. Consistent with the reduction of the BA pool size resulting in a state of low transhepatic BA flow, differential gene expression suggested decreased activation of Fxr, i.e., the expression of Shp, a repressor of BA synthesis pathways, was diminished resulting in increased expression of the rate-limiting enzyme (*Cyp7a1*) for BA synthesis. Importantly, genes encoding proteins with potentially protective properties during cholestasis were also upregulated in SC-435 treated mdr2−/− mice, including *Ppara*, which may promote alternative BA elimination/detoxification and reduce inflammation (3), *Car3* and *Aqp8*, involved in bicarbonate-rich hydrocholeresis reducing the toxic effects of hydrophobic BA on biliary epithelium (32, 33), and *Igf1*, reported to exert antifibrogenic properties in cholestasis (12). In addition, out of the 332 downregulated genes in SC-435 treated mdr2−/− mice, 95 play a role in inflammation and fibrosis, most prominently *Ccl2*/Mcp1 and *Lcn2*/lipocalin 2. Mcp1 is expressed by bile duct epithelial cells upon exposure to BA (34), and has been linked to activation of hepatic stellate cells in biliary atresia and cystic fibrosis (35). Lipocalin 2 is secreted by hepatocytes and involved in leucocyte recruitment, and was found to be a sensitive biomarker of liver injury (36).

Many changes in the hepatic gene expression profile appear consistent with what would be expected to occur when severe cholestasis is alleviated, including Fxr inactivation and reduction of pro-inflammatory gene expression, and might be operative in any cholestatic disorder in which enterohepatic BA uptake is disrupted. Other results of our studies may have more specific bearing for the pathogenesis of sclerosing cholangitis in mdr2−/− mice, in particular our findings on the changes in bile composition. We propose that reduction of biliary BA and cholesterol concentrations, which are determinants of bile solubility and cholangiocyte injury from precipitated bile microcrystals in mdr2−/− mice (9, 10), were critical for attenuation of the sclerosing cholangitis phenotype. We speculate that increased cholehepatic shunting, reported to be the result of bile duct proliferation in mdr2−/− mice (27), and downregulation of genes encoding the canalicular BA and cholesterol transporters Mdr1 and Abcg5, respectively, contribute to this change in bile composition despite activation of *de novo* hepatic BA synthesis following treatment with SC-435. Our findings of decreased frequency of Ki67 expressing cholangiocytes and improved liver ultrastructure with intact basement membranes surrounding interlobular bile ducts may indicate reduced BA leakage and support this mechanism of action of SC-435 in mdr2−/− mice.

Finally, we validated results of gene expression studies which revealed decreased hepatic expression of chemokines recruiting leukocytes to the liver by showing that SC-435 treatment decreased the frequency of Kupffer cells, neutrophils and inflammatory monocytes accompanied by expansion of anti-inflammatory Ly6C- monocytes. Interestingly, this pattern of changes in hepatic leukocyte composition has previously been reported during treatment with a Tgr5 receptor agonist in a model of steatohepatitis (37). This raises the possibility that some of the effects of SC-435 on hepatic inflammation are mediated by Tgr5, as previously described for metabolic effects observed in treatment with anionic resins, an alternative method of disrupting enterohepatic circulation of BA. These studies suggested that binding of BA by resins resulted in spill-over of BA into the colon which led to Tgr5-dependent intestinal release of glucagon-like peptide (Glp)-1 exerting

Author Manuscript Author Manuscript Author Manuscript Author Manuscript

glycemic control in the liver (38). Whether ASBT inhibitors affect Tgr5 signaling in the colon and modulate secretion of Glp-1 requires further investigations.

In summary, this preclinical study demonstrates the potential of pharmacological inhibition of ASBT in halting the progression of fibrosing cholangiopathies during the early phase of the disease process and identifies several mechanisms of action, which may operate synergistically.

Supplementary Material

Refer to Web version on PubMed Central for supplementary material.

Acknowledgments

Financial Support:

The National Institute of Diabetes, Digestive and Kidney Diseases (NIDDK) grant DK095001 and the foundation "PSC Partners seeking a cure" supported this study (to A.G.M.). Lumena Pharmaceutical Inc. (now Shire Plc) provided research funds to A.G.M and K.D.R.S. The project was supported in part by NIH- T32DK007727 to A.T., and PHS Grant P30 DK078392 (Pathology Core, Gene expression Core, Bioinformatics) of the Digestive Disease Research Core Center in Cincinnati and the Research Flow Cytometry Core in the Division of Rheumatology at Cincinnati Children's Hospital Medical Center, supported in part by NIH AR-47363, NIH DK78392 and NIH DK90971. Investigators having affiliations with Lumena Pharmaceutical Inc. or Shire plc. were not involved in the collection of data, analysis, or interpretation of the results.

List of Abbreviations

BA	bile acid
ASBT	apical sodium-dependent bile acid transporter
Mdr2	multi drug resistance 2
PFIC type 3	progressive familial intrahepatic cholestasis type 3
PSC	primary sclerosing cholangitis
PL	phospholipids
PC	phosphatidylcholine
ALT	alanine aminotransferase
ALP	alkaline phosphatase
LC-MS	liquid chromatography-mass spectrometry
DOT	day of treatment

References

1. Beuers U, Trauner M, Jansen P, Poupon R. New paradigms in the treatment of hepatic cholestasis: From UDCA to FXR, PXR and beyond. J Hepatol. 2015; 62:S25–S37. [PubMed: 25920087]
2. Hirschfield GM, Heathcote EJ, Gershwin ME. Pathogenesis of cholestatic liver disease and therapeutic approaches. Gastroenterology. 2010; 139:1481–1496. [PubMed: 20849855]
3. Ghonem NS, Assis DN, Boyer JL. On fibrates and cholestasis: A review. Hepatology. 2015

Author Manuscript Author Manuscript Author Manuscript Author Manuscript

4. Patel T, Gores GJ. Apoptosis and hepatobiliary disease. Hepatology. 1995; 21:1725–1741. [PubMed: 7768518]
5. Karlsen TH, Franke A, Melum E, Kaser A, Hov JR, Balschun T, Lie BA, et al. Genome-wide association analysis in primary sclerosing cholangitis. Gastroenterology. 2010; 138:1102–1111. [PubMed: 19944697]
6. Hoegenauer K, Arista L, Schmiedeberg N, Werner G, Jaksche H, Bouhelal R, Nguyen DG, et al. G-Protein-coupled Bile Acid Receptor 1 (GPBAR1, TGR5) agonists reduce the production of pro-inflammatory cytokines and stabilize the alternative macrophage phenotype. J Med Chem. 2014
7. Gonzales E, Davit-Spraul A, Baussan C, Buffet C, Maurice M, Jacquemin E. Liver diseases related to MDR3 (ABCB4) gene deficiency. Front Biosci. 2009; 14:4242–4256.
8. Trauner M, Fickert P, Baghdasaryan A, Claudel T, Halilbasic E, Moustafa T, Wagner M, et al. New insights into autoimmune cholangitis through animal models. Dig Dis. 2010; 28:99–104. [PubMed: 20460897]
9. Lammert F, Wang DQ, Hillebrandt S, Geier A, Fickert P, Trauner M, Matern S, et al. Spontaneous cholecysto- and hepatolithiasis in Mdr2−/− mice: a model for low phospholipid-associated cholelithiasis. Hepatology. 2004; 39:117–128. [PubMed: 14752830]
10. Fickert P, Fuchsbichler A, Wagner M, Zollner G, Kaser A, Tilg H, Krause R, et al. Regurgitation of bile acids from leaky bile ducts causes sclerosing cholangitis in Mdr2 (Abcb4) knockout mice. Gastroenterology. 2004; 127:261–274. [PubMed: 15236191]
11. Fickert P, Wagner M, Marschall HU, Fuchsbichler A, Zollner G, Tsybrovskyy O, Zatloukal K, et al. 24-norUrsodeoxycholic acid is superior to ursodeoxycholic acid in the treatment of sclerosing cholangitis in Mdr2 (Abcb4) knockout mice. Gastroenterology. 2006; 130:465–481. [PubMed: 16472600]
12. Stiedl P, McMahon R, Blaas L, Stanek V, Svinka J, Grabner B, Zollner G, et al. Growth hormone resistance exacerbates cholestasis-induced murine liver fibrosis. Hepatology. 2015; 61:613–626. [PubMed: 25179284]
13. West KL, Ramjiganesh T, Roy S, Keller BT, Fernandez ML. 1-[4-[4[(4R,5R)-3,3-Dibutyl-7-(dimethylamino)-2,3,4,5-tetrahydro-4-hydroxy-1,1-di oxido-1-benzothiepin-5-yl]phenoxy]butyl]-4-aza-1-azoniabicyclo[2.2.2]octane methanesulfonate (SC-435), an ileal apical sodium-codependent bile acid transporter inhibitor alters hepatic cholesterol metabolism and lowers plasma low-density lipoprotein-cholesterol concentrations in guinea pigs. J Pharmacol Exp Ther. 2002; 303:293–299. [PubMed: 12235263]
14. Lages CS, Simmons J, Chougnet CA, Miethke AG. Regulatory T cells control the CD8 adaptive immune response at the time of ductal obstruction in experimental biliary atresia. Hepatology. 2012; 56:219–227. [PubMed: 22334397]
15. Hagio M, Matsumoto M, Fukushima M, Hara H, Ishizuka S. Improved analysis of bile acids in tissues and intestinal contents of rats using LC/ESI-MS. J Lipid Res. 2009; 50:173–180. [PubMed: 18772484]
16. He H, Mennone A, Boyer JL, Cai SY. Combination of retinoic acid and ursodeoxycholic acid attenuates liver injury in bile duct-ligated rats and human hepatic cells. Hepatology. 2011; 53:548–557. [PubMed: 21274875]
17. Macri SC, Bailey CC, de Oca NM, Silva NA, Rosene DL, Mansfield KG, Miller AD. Immunophenotypic alterations in resident immune cells and myocardial fibrosis in the aging rhesus macaque (Macaca mulatta) heart. Toxicol Pathol. 2012; 40:637–646. [PubMed: 22328408]
18. Trapnell C, Pachter L, Salzberg SL. TopHat: discovering splice junctions with RNA-Seq. Bioinformatics. 2009; 25:1105–1111. [PubMed: 19289445]
19. Trapnell C, Williams BA, Pertea G, Mortazavi A, Kwan G, van Baren MJ, Salzberg SL, et al. Transcript assembly and quantification by RNA-Seq reveals unannotated transcripts and isoform switching during cell differentiation. Nat Biotechnol. 2010; 28:511–515. [PubMed: 20436464]
20. Chen J, Bardes EE, Aronow BJ, Jegga AG. ToppGene Suite for gene list enrichment analysis and candidate gene prioritization. Nucleic Acids Res. 2009; 37:W305–311. [PubMed: 19465376]
21. Galman C, Arvidsson I, Angelin B, Rudling M. Monitoring hepatic cholesterol 7alpha-hydroxylase activity by assay of the stable bile acid intermediate 7alpha-hydroxy-4-cholesten-3-one in peripheral blood. J Lipid Res. 2003; 44:859–866. [PubMed: 12562858]

Author Manuscript Author Manuscript Author Manuscript Author Manuscript

22. Hofmann AF. Bile acid secretion, bile flow and biliary lipid secretion in humans. Hepatology. 1990; 12:17S–22S. discussion 22S-25S. [PubMed: 2210645]
23. Hofmann AF, Small DM. Detergent properties of bile salts: correlation with physiological function. Annu Rev Med. 1967; 18:333–376. [PubMed: 5337530]
24. Wang DQ, Carey MC. Complete mapping of crystallization pathways during cholesterol precipitation from model bile: influence of physical-chemical variables of pathophysiologic relevance and identification of a stable liquid crystalline state in cold, dilute and hydrophilic bile salt-containing systems. J Lipid Res. 1996; 37:606–630. [PubMed: 8728323]
25. Golbar HM, Izawa T, Wijesundera KK, Tennakoon AH, Katou-Ichikawa C, Tanaka M, Kuwamura M, et al. Expression of nestin in remodelling of alpha-naphthylisothiocyanate-induced acute bile duct injury in rats. J Comp Pathol. 2014; 151:255–263. [PubMed: 25087881]
26. West KL, Zern TL, Butteiger DN, Keller BT, Fernandez ML. SC-435, an ileal apical sodium co-dependent bile acid transporter (ASBT) inhibitor lowers plasma cholesterol and reduces atherosclerosis in guinea pigs. Atherosclerosis. 2003; 171:201–210. [PubMed: 14644388]
27. Hulzebos CV, Voshol PJ, Wolters H, Kruit JK, Ottenhof R, Groen AK, Stellaard F, et al. Bile duct proliferation associated with bile salt-induced hypercholeresis in Mdr2 P-glycoprotein-deficient mice. Liver Int. 2005; 25:604–612. [PubMed: 15910498]
28. van Nieuwerk CM, Groen AK, Ottenhoff R, van Wijland M, van den Bergh Weerman MA, Tytgat GN, Offerhaus JJ, et al. The role of bile salt composition in liver pathology of mdr2 (−/−) mice: differences between males and females. J Hepatol. 1997; 26:138–145. [PubMed: 9148004]
29. Billington D, Evans CE, Godfrey PP, Coleman R. Effects of bile salts on the plasma membranes of isolated rat hepatocytes. Biochem J. 1980; 188:321–327. [PubMed: 7396866]
30. Faubion WA, Guicciardi ME, Miyoshi H, Bronk SF, Roberts PJ, Svingen PA, Kaufmann SH, et al. Toxic bile salts induce rodent hepatocyte apoptosis via direct activation of Fas. J Clin Invest. 1999; 103:137–145. [PubMed: 9884343]
31. Yerushalmi B, Dahl R, Devereaux MW, Gumpricht E, Sokol RJ. Bile acid-induced rat hepatocyte apoptosis is inhibited by antioxidants and blockers of the mitochondrial permeability transition. Hepatology. 2001; 33:616–626. [PubMed: 11230742]
32. Banales JM, Prieto J, Medina JF. Cholangiocyte anion exchange and biliary bicarbonate excretion. World J Gastroenterol. 2006; 12:3496–3511. [PubMed: 16773707]
33. Beuers U, Hohenester S, de Buy Wenniger LJ, Kremer AE, Jansen PL, Elferink RP. The biliary HCO(3)(-) umbrella: a unifying hypothesis on pathogenetic and therapeutic aspects of fibrosing cholangiopathies. Hepatology. 2010; 52:1489–1496. [PubMed: 20721884]
34. Lamireau T, Zoltowska M, Levy E, Yousef I, Rosenbaum J, Tuchweber B, Desmouliere A. Effects of bile acids on biliary epithelial cells: proliferation, cytotoxicity, and cytokine secretion. Life Sci. 2003; 72:1401–1411. [PubMed: 12527037]
35. Ramm GA, Shepherd RW, Hoskins AC, Greco SA, Ney AD, Pereira TN, Bridle KR, et al. Fibrogenesis in pediatric cholestatic liver disease: role of taurocholate and hepatocyte-derived monocyte chemotaxis protein-1 in hepatic stellate cell recruitment. Hepatology. 2009; 49:533–544. [PubMed: 19115220]
36. Labbus K, Henning M, Borkham-Kamphorst E, Geisler C, Berger T, Mak TW, Knuchel R, et al. Proteomic profiling in Lipocalin 2 deficient mice under normal and inflammatory conditions. J Proteomics. 2013; 78:188–196. [PubMed: 23219901]
37. McMahan RH, Wang XX, Cheng LL, Krisko T, Smith M, El Kasmi K, Pruzanski M, et al. Bile acid receptor activation modulates hepatic monocyte activity and improves nonalcoholic fatty liver disease. J Biol Chem. 2013; 288:11761–11770. [PubMed: 23460643]
38. Harach T, Pols TW, Nomura M, Maida A, Watanabe M, Auwerx J, Schoonjans K. TGR5 potentiates GLP-1 secretion in response to anionic exchange resins. Sci Rep. 2012; 2:430. [PubMed: 22666533]

Author Manuscript Author Manuscript Author Manuscript Author Manuscript

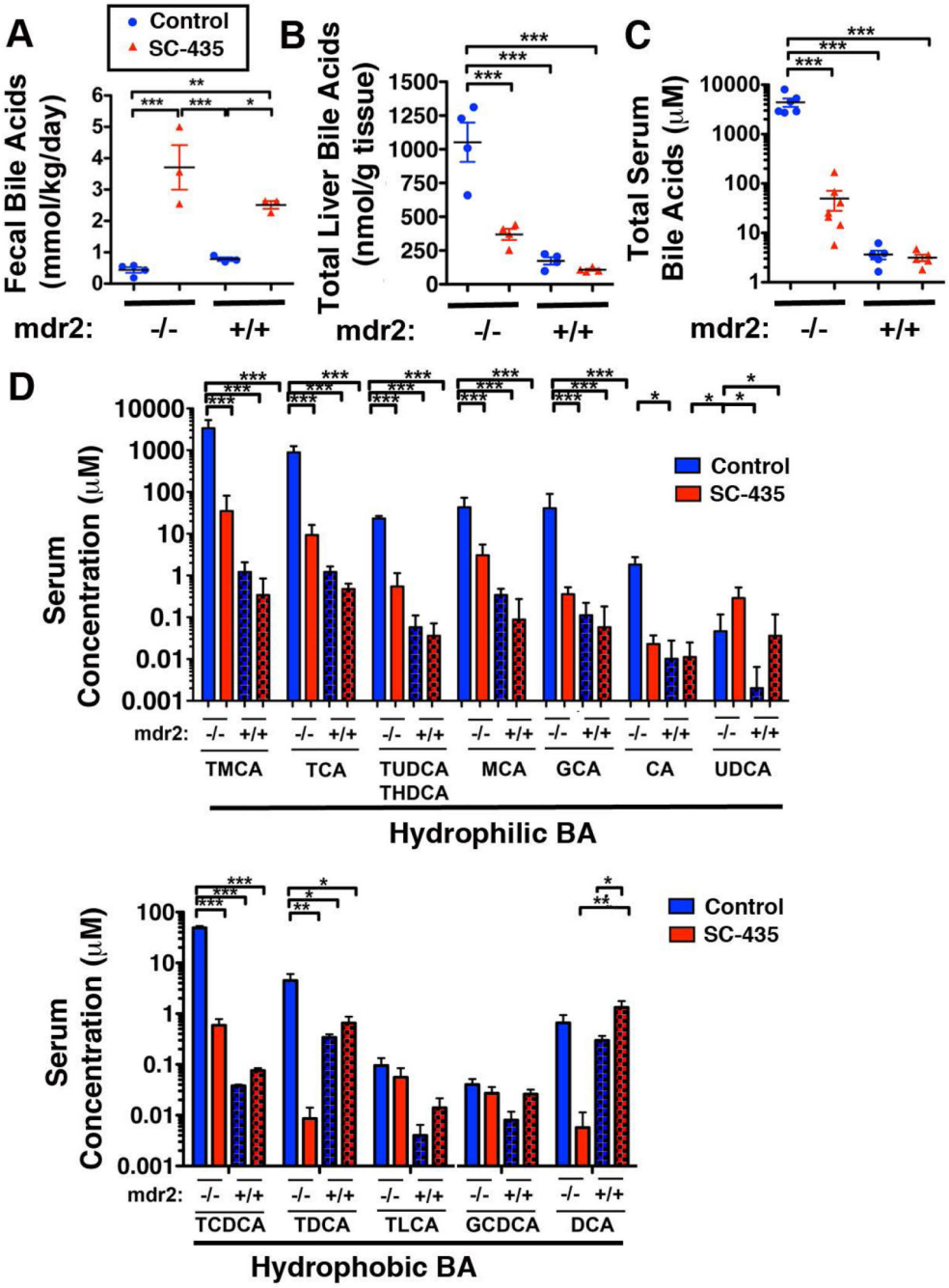

Figure 1. SC-435 increases fecal BA excretion and lowers liver and serum BA levels in mdr2−/− mice

30-day-old female mdr2−/− and age- and sex-matched mdr2+/+ received chow (Lab 5020) containing 0.006% SC-435, or the same chow without the compound (controls). Feces were collected for 48 hours prior to day of treatment (DOT) 14; BA were extracted and subjected to enzymatic quantification (**A**). Concentrations of individual BA in liver and serum samples, collected on DOT 14, were determined by tandem mass spectrometry, and plotted as total liver and serum BA concentration in **B** and **C**, respectively**.** Individual species were

Author Manuscript Author Manuscript Author Manuscript Author Manuscript

grouped as hydrophilic and hydrophobic BAs in **D**. Statistical analysis: one-way ANOVA with Tukey's multiple comparison test was applied to the data, with *, **, *** denoting p-values of <0.05, <0.01, <0.001, respectively.

Author Manuscript Author Manuscript Author Manuscript Author Manuscript

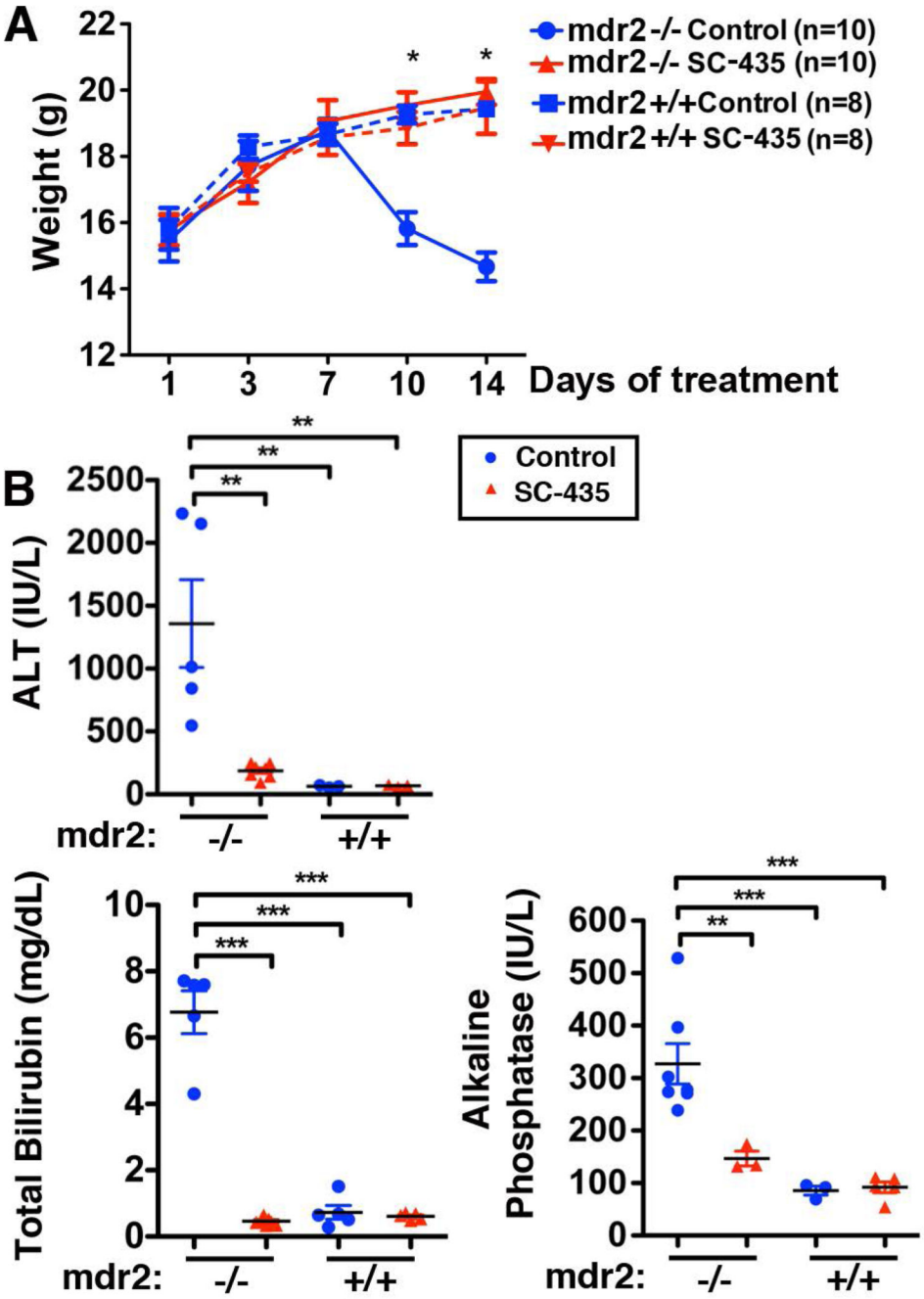

Figure 2. SC-435 prevents wasting and reduces biomarkers of hepatocellular injury and cholestasis in mdr2−/− mice

Body weights were recorded for mice of the four groups during the 14 days of intervention (**A**). ALT, total bilirubin, and alkaline phosphatase levels were determined on blood sampled by cardiocentesis on DOT 14. Statistical analysis: unpaired t test was applied to the data from treated and control mdr2−/− mice in **A**, one-way ANOVA with Tukey's multiple comparison test in **B.**

Author Manuscript Author Manuscript Author Manuscript Author Manuscript

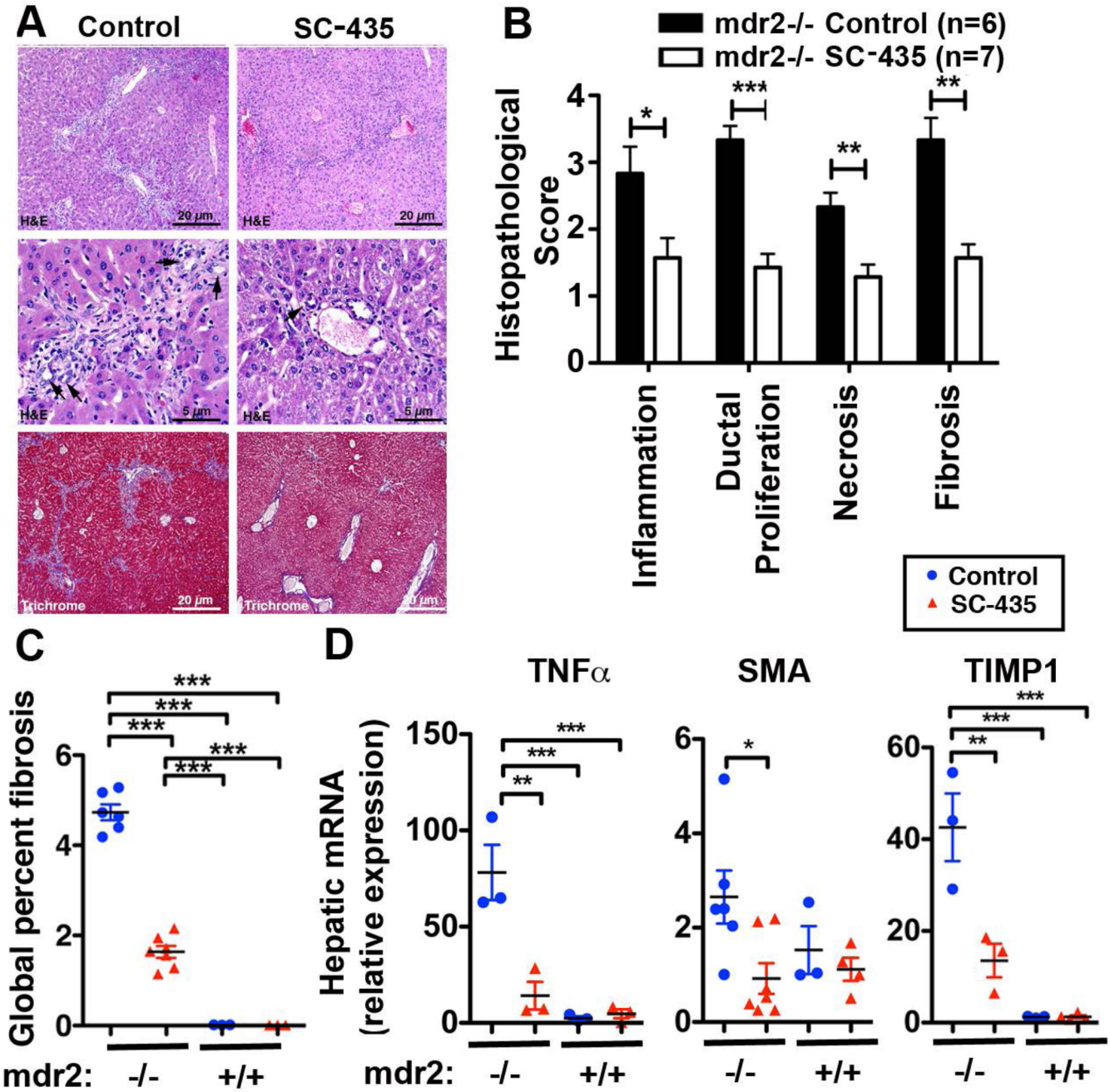

Figure 3. SC-435 treatment is associated with reduced periportal inflammation and fibrosis in mdr2−/− mice

Sections from paraffin embedded liver samples obtained from mdr2−/− mice on DOT 14 were subjected to H&E and Trichrome staining. Representative photomicrographs of sections are shown in **A**, with arrowheads denoting bile duct profiles. The components of sclerosing cholangitis score (inflammation, ductal proliferation, necrosis, and fibrosis) were analyzed on a 1 to 4+ scale (**B**). Trichrome stained slides from livers of SC-435-treated and control mdr2−/− mice were subjected to automated Aperio-based tissue image analysis to quantify the percentage of liver fibrosis (**C**). Total hepatic RNA from 44-day old mice of the

Author Manuscript Author Manuscript Author Manuscript Author Manuscript

four groups was subjected to qPCR and relative expression of the pro-inflammatory gene *TNFα* and of the profibrogenic genes *SMA* and *TIMP1* was computed by ΔΔCT analysis using HPRT as the house keeping gene (**D**). Statistical analysis: unpaired t test was applied to the data of the two groups (SC-435 vs control) in mdr2−/− mice in **B**, with *, **, *** denoting p-values of <0.05, <0.01, <0.001, respectively, and one-way ANOVA in **C** and **D**.

Author Manuscript Author Manuscript Author Manuscript Author Manuscript

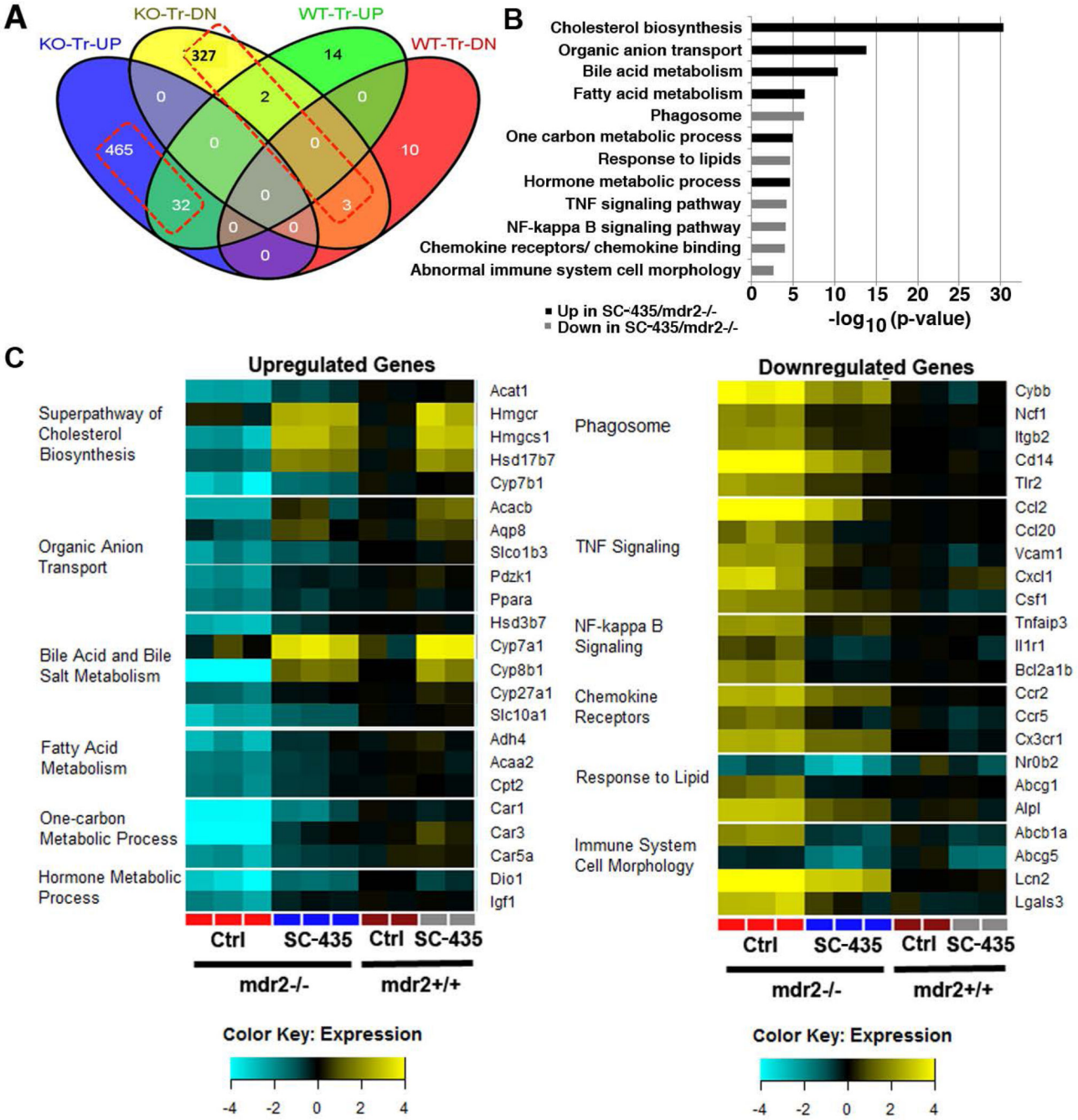

Figure 4. SC-435 treatment is associated with hepatic upregulation of genes controlling BA pool size and putative hepatoprotective genes and downregulation of pro-inflammatory genes

RNAseq studies were performed on total hepatic RNA from mice of the four treatment groups. Distribution of up- and downregulated genes (>2-fold difference) compared to untreated mice of the respective genotype (knockout [KO] and wild type [WT]) across the different treatment groups is depicted in a Venn diagram (**A**). Based on pathway enrichment analysis, 12 pathways comprising significantly up- or downregulated genes in SC-435 treated mdr2−/− compared to mdr2−/− control mice are depicted with p values for these

Author Manuscript Author Manuscript Author Manuscript Author Manuscript

pathways plotted as $-\log_{10}$ (**B**). 23 genes from the up- and downregulated pathways, respectively, are displayed in the heatmaps with expression levels normalized to control mdr2+/+ mice (**C).**

Author Manuscript Author Manuscript Author Manuscript Author Manuscript

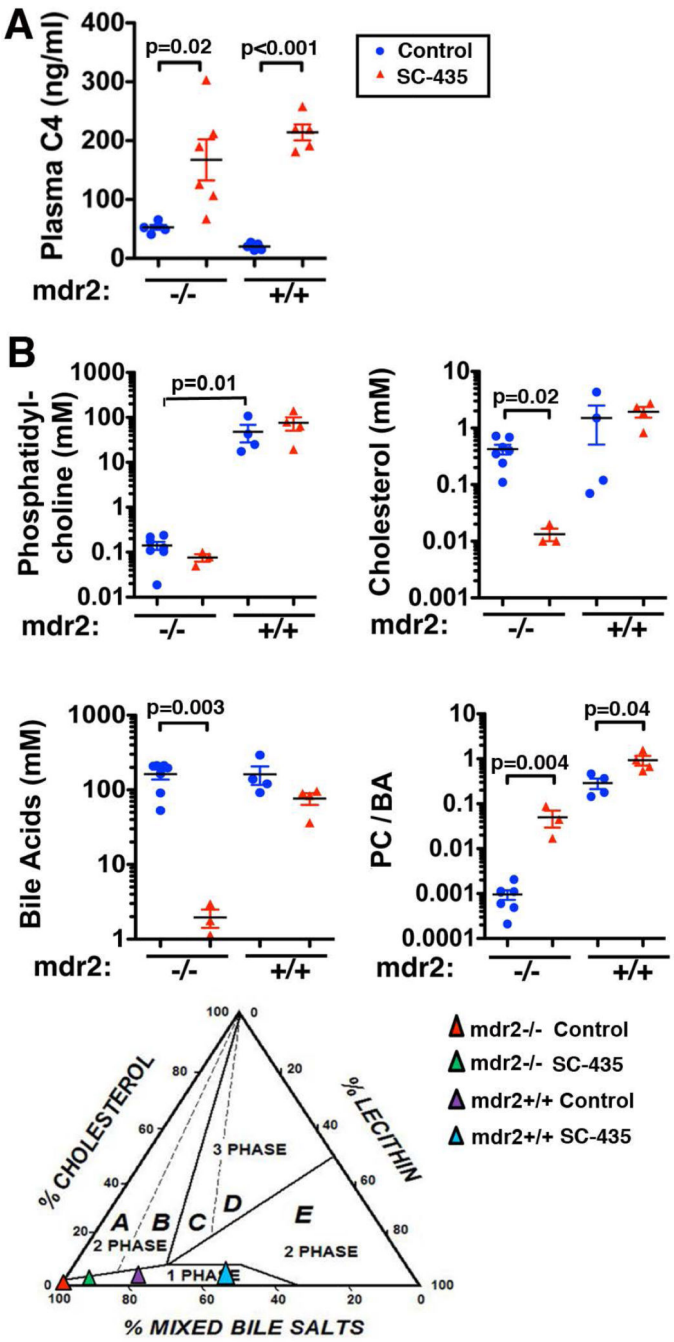

Figure 5. Despite increase in hepatic BA synthesis rate, SC-435 treatment is associated with reduced biliary BA concentration

Concentrations for the biological precursor 7α-hydroxy-4-cholesten-3-one (C4), which correlates with BA synthesis, were determined by tandem mass spectrometry in plasma samples obtained on DOT 14 (**A**). Bile was aspirated from the gallbladders on DOT14 and subjected to MS-based quantification of PC, cholesterol, and BA concentrations. The biliary molar ratios of PC/BA (linkage coefficient) were calculated based on these measurements, and mean values of the bile constituents were plotted in a ternary phase diagram. Control

Author Manuscript Author Manuscript Author Manuscript Author Manuscript

mdr2−/− mice plot in region A, which is a 2 phase zone of the Wang and Carey diagram, characterized by very low PC/BA ratio, cholesterol supersaturation and formation of cholesterol crystals. SC-435 treated mdr2−/− and both groups of wild type mice plot in the micellar 1 phase zone of the diagram (**B**). Statistical analysis: unpaired t test was applied to compare the data between the two groups (SC-435 vs control) in mdr2−/− and mdr2+/+ mice.

Author Manuscript Author Manuscript Author Manuscript Author Manuscript

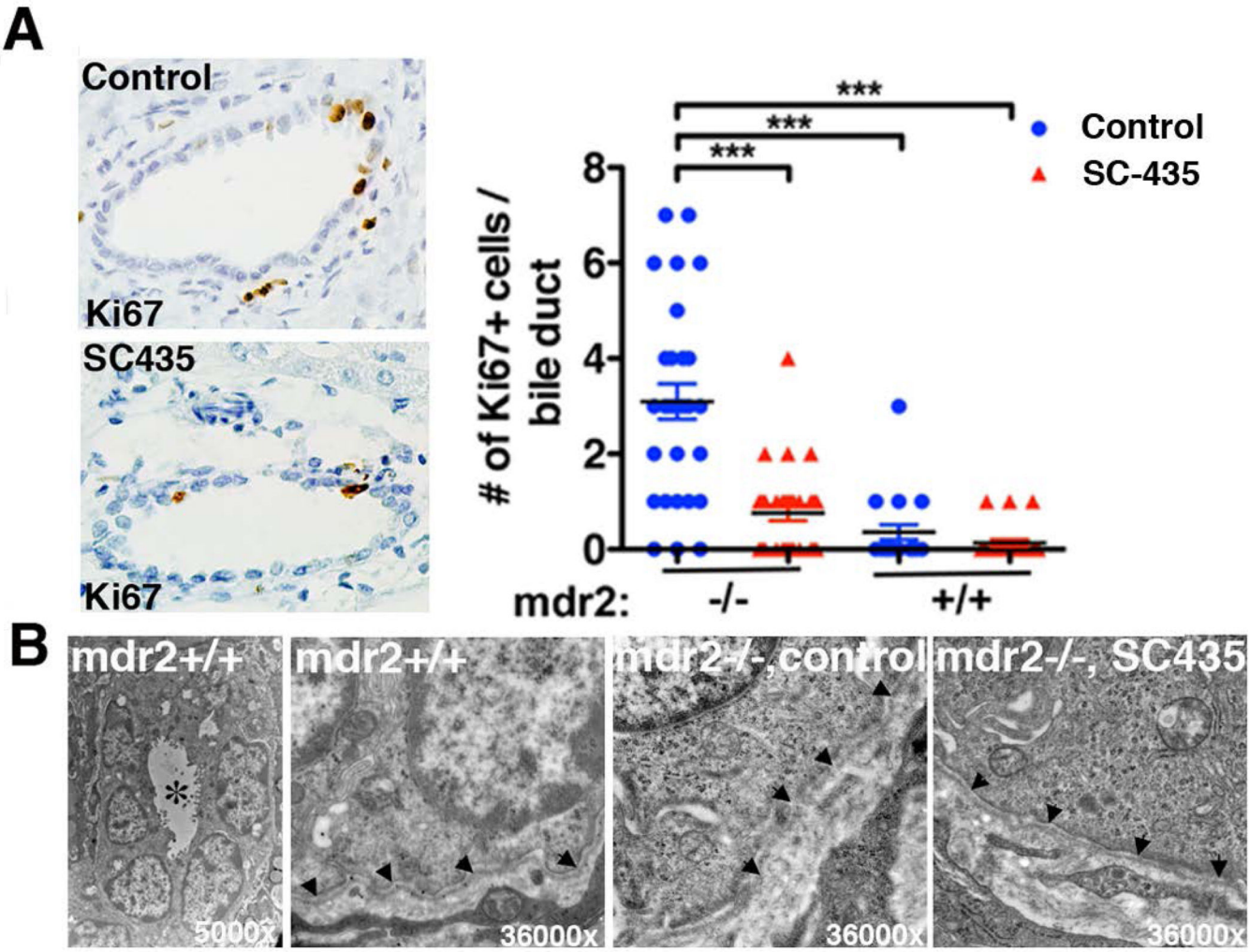

Figure 6. SC-435 treatment is associated with decreased bile duct epithelial injury and partial restoration of ultrastructural integrity

Paraffin-embedded liver sections from SC-435 treated and control mice (n=2-3/group) were subjected to Ki67 immunohistochemistry. Ki67 positive cells were enumerated in large interlobular bile ducts (10 bile duct profiles/ liver). Statistical analysis: one-way ANOVA was applied to compare the data between the groups (**A**). In **B**, glutaraldehyde-fixed liver sections were analyzed by electron microscopy. Left panel depicts a bile duct profile in control mdr2+/+ mice in low magnification, with * denoting the lumen. The other images show higher magnification of the basement membrane (denoted by arrowheads) in mdr2+/+ mice, which is disrupted in control mdr2−/− mice; integrity is restored in SC-435-treated mdr2−/− mice. 10 bile duct profiles were examined per group (n=2 mice/group), of which 4 were surrounded by intact basement membrane in control and 7 in SC-435 treated mice.

Author Manuscript Author Manuscript Author Manuscript Author Manuscript

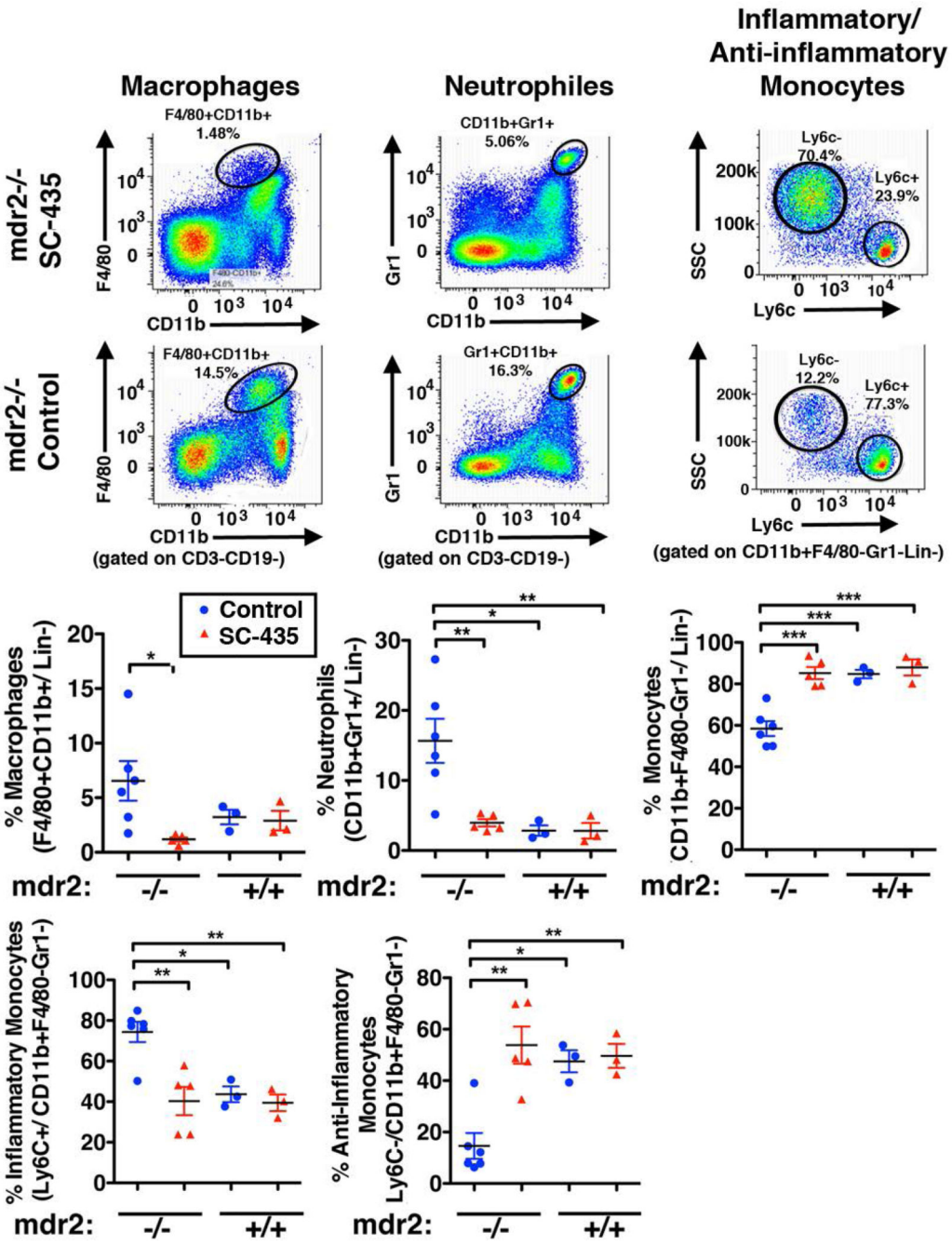

Figure 7. SC-435 treatment is associated with decreased population of the liver with macrophages, neutrophils and a shift towards anti-inflammatory monocytes

Single cell suspensions were prepared from livers of mice from the four treatment groups and subjected to flow cytometry. The two top panels delineate the gating strategies: Following out-gating of cell duplets, debris and lineage positive $CD3^+$ or $CD19^+$ cells, macrophages (Kupffer cells) were identified as $F4/80^+CD11b^+$ and neutrophils as $Gr1^{high}CD11b^+$ cells. $F4/80^-$ and $Gr1^-$ $CD11b^+$ myeloid were further distinguished into inflammatory ($Ly6C^+$) and anti-inflammatory ($Ly6C^-$) monocytes. Frequencies of these cell

populations were enumerated as denoted in the graphs, and differences in means between the groups were tested for statistical significance with one-way ANOVA.

Author Manuscript Author Manuscript Author Manuscript Author Manuscript